Title
Simulations of Plug-in Hybrid Vehicles Using Advanced Lithium Batteries and Ultracapacitors on Various Driving Cycles

Permalink
https://escholarship.org/uc/item/4wb3g744

Authors
Burke, Andy
Zhao, Hengbing

Publication Date
2010

Simulations of Plug-in Hybrid Vehicles using Advanced Lithium Batteries and Ultracapacitors on Various Driving Cycles

Andrew Burke
Hengbing Zhao

University of California-Davis
Institute of Transportation Studies

Abstract

The use of ultracapacitors in plug-in hybrid vehicles (PHEVs) with high energy density lithium-ion and zinc-air batteries is studied. Simulations were performed for various driving cycles with the PHEVs operating in the charge depleting and charge sustaining modes. The effects of the load leveling of the power demand from the batteries using the ultracapacitors are evident. The average and the peak currents from the batteries are lower by a factor of 2-3.

Introduction

Simulation models [1-3] of hybrid-electric vehicles using *Advisor* have been prepared at the University of California-Davis, Institute of Transportation Studies. The hybrid-electric drivelines modeled included the Honda single-shaft, Toyota planetary, GM two-mode, and the VW/Borg Warner dual clutch transmission arrangements. Both charge sustaining HEV and plug-in hybrid vehicles have been simulated using nickel metal hydride and lithium-ion batteries. In the present study, the simulation models have been extended to include the cases of battery/ultracapacitor combinations for energy storage (2-energy storage systems and associated control strategies). These new models include DC/DC inverters to control the energy flow from the battery and/or the ultracapacitors. The control strategies result in load leveling the batteries and having the ultracapacitors accept all the regenerative braking energy. This paper is concerned with the application of the 2-energy storage models to plug-in hybrid vehicles (PHEV) using advanced lithium batteries having energy densities of 200-400 Wh/kg. These high energy density batteries often do not have commensurate high power capability and thus will benefit greatly by being combined with ultracapacitors or other very high power capability devices. This is especially true of PHEV designs which are intended for all-electric operation in the charge depleting mode. In this paper, simulation results are presented for mid-size PHEVs with all-electric ranges of 25-90 km. It is shown that high energy density, relatively low power batteries combined with ultracapacitors will provide good all-electric vehicle performance with much reduced stress on the batteries. This is expected to significantly enhance battery cycle life.

Battery and Ultracapacitor Characteristics

A number of lithium batteries and ultracapacitors have been tested in the laboratory at the University of California-Davis [4-7]. A summary of the test results for the batteries is given in Table 1 and for the ultracapacitors in Table 2. For both energy storage technologies, the devices with the highest energy density typically have the lowest power capability. The pulse power capabilities shown in the tables were calculated using the following relationships:

$$\text{Batteries:} \quad P = EF(1-EF) \, V_{oc}^2 / R$$
$$\text{Ultracapacitors:} \quad P = 9/16(1-EF) \, V_{rated}^2 / R$$

where EF is the efficiency of the pulse (EF= V_{pulse} / V_{oc}).

The matched impedance power which is often cited for both battery and ultracapacitor devices is calculated as follows:

$$P_{match\ imped.} = V^2 / 4R$$

For charge sustaining hybrids, it seems reasonable to cite the power capability of devices for pulse power efficiencies of 90-95%. For PHEVs and EVs operating in charge depleting modes for the battery, it is reasonable to cite the power for efficiencies of 75-80%. In all instances, the power capability is proportional to V^2/R so that high power capability requires a low resistance R.

Batteries

The primary goal of this paper is to investigate via vehicle modeling the performance of combinations of advanced batteries and ultracapacitors in PHEVs and compare that performance with the batteries alone. Vehicle simulations are performed for batteries having a wide range of energy densities and power capabilities. The characteristics of some of the batteries are based on cell test data [4-7] while the characteristics of others are those of projected (fictitious) cells of advanced chemistries. A summary of the characteristics of the batteries used in the vehicle simulations is given in Table 3. The batteries were projected to have energy densities between 200 and 400 Wh/kg and varying power capability.

Little direct information is given in the literature concerning the energy density of particular cell designs using advanced materials such as MnO2 composites and silicone carbon composites. Electrode material properties are given based on electrode test data [8-11], but as yet no test data on cells assembled using the materials seems to be available in the literature. Hence the cell performance values given in Table 3 are only estimates selected to show the effect of the cell performance on PHEV performance with and without the use of ultracapacitors. The resistances and power capabilities shown in Table 3 for the advanced lithium battery chemistries are based on extrapolating the Ah-mOhm values from the resistance test data shown in Table 1. The power densities for 95% and 75% pulses were calculated using the equation for battery power previously discussed.

Table 1: Summary of the performance characteristics of lithium-ion batteries of various chemistries

Battery Developer/ Cell type	Electrode chemistry	Voltage range	Ah	Resist. mOhm	Wh/kg	W/kg 90% effic.*	W/kg Match. Imped.	Wgt. (kg)	Density gm/cm3
Enerdel HEV	Graphite/ Ni MnO2	4.1-2.5	15	1.4	115	2010	6420	.445	----
Enerdel EV/PHEV	Graphite/ Ni MnO2	4.1-2.5	15	2.7	127	1076	3494	.424	----
Kokam prismatic	Graphite/ NiCoMnO2	4.1-3.2	30	1.5	140	1220	3388	.787	2.4
Saft Cylind.	Graphite/ NiCoAl	4.0-2.5	6.5	3.2	63	1225	3571	.35	2.1
GAIA Cylind.	Graphite/ NiCoMnO2	4.1-2.5	40 / 7	.48 / 3.6	96 / 78	2063	5446 / 3472	1.53 / .32	3.22 / ---
A123 Cylind.	Graphite/Iron Phosph.	3.6-2.0	2.2	12	90	1393	3857	.07	2.2
Altairnano prismatic	LiTiO/ NiMnO2	2.8-1.5	11	2.2	70	990	2620	.34	1.83
Altairnano prismatic	LiTiO/ NiMnO2	2.8-1.5	3.8	1.15	35	2460	6555	.26	1.91
Quallion Cylind.	Graphite/ NiCo	4.2-2.7	1.8	60	144	577	1550	.043	2.6
Quallion Cylind.	Graphite/ NiCo	4.2-2.7	2.3	72	170	445	1182	.047	2.8
EIG prismatic	Graphite/ NiCoMnO2	4.2-3.0	20	3.1	165	1278	3147	.41	----
EIG prismatic	Graphite/Iron Phosph.	3.65-2.0	15	2.5	113	1100	3085	.42	---
Panasonic EV prismatic	Ni Metal hydride	7.2-5.4	6.5	11.4	46	395	1093	1.04	1.8

* power density $P = \text{Eff.} \cdot (1-\text{Eff.}) \, V_{oc}^2/R$, $P_{match.\ imped.} = V^2/4R$

Table 2: Summary of ultracapacitor device characteristics

Device	V rated	C (F)	R (mOhm)	RC (sec)	Wh/kg (1)	W/kg (95%) (2)	W/kg Match. Imped.	Wgt. (kg)	Vol. lit.
Maxwell*	2.7	2885	.375	1.08	4.2	994	8836	.55	.414
Maxwell	2.7	605	.90	.55	2.35	1139	9597	.20	.211
Skeleton Technologies	2.8	1600	1.3	2.1	5.8	800	7140	.22	.13
ApowerCap**	2.7	55	4	.22	5.5	5695	50625	.009	---
Apowercap**	2.7	450	1.3	.58	5.89	2766	24595	.057	.045
Ness	2.7	1800	.55	1.00	3.6	975	8674	.38	.277
Ness	2.7	3640	.30	1.10	4.2	928	8010	.65	.514
Ness (cyl.)	2.7	3160	.4	1.26	4.4	982	8728	.522	.379
Asahi Glass (propylene carbonate)	2.7	1375	2.5	3.4	4.9	390	3471	.210 (estimated)	.151
Panasonic (propylene carbonate)	2.5	1200	1.0	1.2	2.3	514	4596	.34	.245
EPCOS	2.7	3400	.45	1.5	4.3	760	6750	.60	.48
LS Cable	2.8	3200	.25	.80	3.7	1400	12400	.63	.47
BatScap	2.7	2680	.20	.54	4.2	2050	18225	.50	.572
Power Sys. (activated carbon, propylene carbonate) **	2.7	1350	1.5	2.0	4.9	650	5785	.21	.151
Power Sys. (graphitic carbon, propylene carbonate) **	3.3 3.3	1800 1500	3.0 1.7	5.4 2.5	8.0 6.0	486 776	4320 6903	.21 .23	.15 .15
JSR Micro (AC/graphitic carbon)	3.8	1000 2000	4 1.9	4 3.8	11.2 12.1	900 1038	7987 9223	.113 .206	.073 .132

(1) Energy density at 400 W/kg constant power, Vrated - 1/2 Vrated
(2) Power based on P=9/16*(1-EF)*V2/R, EF=efficiency of discharge
   * Except where noted, all the devices use acetonitrile as the electrolyte
   ** All device except those with ** are packaged in metal containers

The resistance and thus the power capability of the rechargeable Zinc-air battery were estimated based on the resistance of a 10Ah cell being developed by Revolt Technology [12] in Switzerland and assuming a large reduction (a factor of about three) in a the Ah-mOhm value of 20Ah cell. As indicated in Table 3, the Zinc-air battery is assumed to be a high energy density, relatively low power technology for vehicle applications. The low power capability of the Zinc-air battery is due to a large extent to its low cell voltage (1.35V) compared to the lithium cells.

Ultracapacitors

The characteristics of power devices are also shown in Table 3. The values shown for the ultracapacitors are for a device using activated carbon in both electrodes and acetonitrile as the electrolyte. The cell performance shown in Table 3 is the present state-of-the art for ultracapacitors based on test data for the ApowerCap 450F device (Table 2). Further improvements in power density are likely, but not assumed in the present study. Higher energy density ultracapacitors are available, but they have lower power capability. In addition to high power density, the carbon/carbon ultracapacitors have a cycle life of

hundreds of thousands of deep discharge cycles. This long cycle life is essential for the present PHEV application.

Table 3: Characteristics of present and future battery cell technologies for EVs and PHEVs

Chemistry Anode/cathode	Cell voltage Max/nom.	Ah	Wgt. kg	R mOhm	EV Wh/kg	HEV W/kg 95%	EV W/kg 75%	Cycle life (deep)	Thermal stability
Present technology batteries									
Graphite/ NiCoMnO$_2$	4.2/3.6	30	.787	1.5	140	521	2060	2000-3000	fairly stable
Graphite/ Mn spinel	4.0/3.6	15	.424	2.7	127	540	2120	1500	fairly stable
Future technology batteries									
Graphite/ composite MnO$_2$	4/3.6	5	.09	20	200	250	1350	----	fairly stable
Silicon carbon composites/ composite MnO$_2$	4/3.6	20	.24	4.5	295	621	2250	---	fairly stable
Rechargeable Zinc-Air	1.3/1.15	20	60	6.6	385	156	616	----	very stable
Present Technology Power devices									
supercapacitor Activated carbon/activated carbon	2.7/1.35	500 F	.068	1.3	5.5	2320	11600	500K	Very stable
Power battery Lithium titanate oxide	2.8/2.5	4	.23	1.15	40	1310	5170	20-50 K	Very stable

Another possible power device technology is a lithium-ion battery using lithium titanate oxide (LTO) in the negative electrode. As indicated in Table 1, cells using LTO have lower energy density than lithium batteries using other chemistries, but they can have significantly higher power and much longer cycle life. Hence for vehicle applications for which energy storage requirements exceed those doable with ultracapacitors, the LTO lithium battery should be considered. The characteristics of LTO cells are included in Table 3, but PHEV simulations using those cells were not done as part of the present study.

Combinations of batteries and ultracapacitors

Next consider the combination of high energy density batteries with ultracapacitors in PHEVs [13]. It will be assumed that the battery is sized by the energy requirement to achieve a specified all-electric range (AER) in the charge depletion mode of operating the vehicle. The energy storage and battery weight for AER between 10 and 40 miles (16-60 km) are shown in Table 4 for battery energy densities between 100-300 Wh/kg. The corresponding power density requirements for 50 and 70 kW electric drivelines in the vehicles are also shown in the table. The power density values shown are high –several kW/kg in some cases- indicating that it is unlikely the high energy density batteries alone will be able to satisfy the power requirements. Hence it seems appropriate to consider combining the batteries with ultracapacitors for the PHEV designs. The results of utilizing a 100 Wh useable energy ultracapacitor pack (20 kg of cells) are shown in Table 5. In these designs, the ultracapacitors can provide a high fraction of the peak power and the batteries the average power that is much lower. This approach to load leveling of the batteries is followed in the vehicle simulations discussed in the next section. Note in Table 5 that for a given AER, the

combined weight of the batteries and ultracapacitors is the lowest using the highest energy density batteries which would not be possible without incorporating the ultracapacitors in the system.

Table 4: Battery sizing and power density for various ranges and motor power

Battery energy density				300 Wh/kg			200 Wh/kg			100Wh/kg	
Range miles	kWh *needed	kWh** stored	** kg	50 kW kW/kg	70kW kW/kg	kg	50kW kW/kg	70kW kW/kg	kg	50kW kW/kg	70kW kW/kg
10	2.52	3.6	12	4.17	5.83	18	2.78	3.89	36	1.39	1.94
15	3.78	5.4	18	2.78	3.89	27	.1.85	2.59	54	.92	1.30
20	5.04	7.2	24	2.08	2.92	36	.1.39	1.94	72	.69	.97
30	7.56	10.8	36	.1.39	1.94	54	. 93	1.30	108	.46	.65
40	10.1	14.4	48	1.04	1.46	72	. .69	.97	144	.35	.49

* Vehicle energy useage from the battery: 250 Wh/mi
** Useable state-of-charge for batteries: 70%, weights shown are for cells only

Table 5: Storage unit weights using a combination of batteries and ultracapacitors for various all-electric ranges

Wh/kg	5	300		200		100	
Range miles	Ultracap kg *	Battery Kg**	Combination kg	Battery kg	Combination kg	Battery kg	Combination kg
10	20	12	32	18	38	36	56
15	20	18	38	27	47	54	74
20	20	24	44	36	56	72	92
30	20	36	56	54	74	108	128
40	20	48	68	72	92	144	164

* The ultracapacitor unit stores 100 Wh useable energy
** Weights shown are for cells only, packaging into modules not included

Modeling of PHEVs Combining Batteries and Ultracapacitors

It has been recognized for a number of years that combining batteries and ultracapacitors can offer advantages in hybrid vehicles [13-20]. Ultracapacitors can deliver very high power and respond in fractions of a second, but have limited storage capacity (100-200 Wh). Batteries have lower power capability, but with high energy density can store relatively large kWh of energy. The combination of batteries and ultracapacitors can deliver high power and high energy and is ideal for PHEVs in term of extending the battery life and downsizing battery pack.

Simulation models of hybrid-electric vehicles using *Advisor* have been prepared at the University of California-Davis, Institute of Transportation Studies [1-3]. The hybrid-electric drivelines modeled included the Honda single-shaft, Toyota planetary, GM two-mode, and the VW/Borg Warner dual clutch transmission arrangements. Both charge sustaining HEV and plug-in hybrid vehicles have been simulated using nickel metal hydride and lithium-ion batteries. As discussed in this section of the paper, the simulation models are extended to include the cases of battery/ultracapacitor combinations for energy storage (2-energy storage systems and associated control strategies). These new models include DC/DC inverters to control the energy flow from the battery and/or the ultracapacitors.   The control strategies result in load leveling the batteries and having the ultracapacitors accept all the regenerative braking energy.

Figure 1 shows topologies of interfacing batteries and ultracapacitors with the motor drive dc-link using a bi-directional dc-dc converter. Figure 1(a) has ultracapacitors directly coupled with the motor drive dc-link. The battery interfaces with the dc-link via a bi-directional dc/dc converter. This topology is well suited for blending ultracapacitors with optimal engine operation. There is a relatively wide variation of the dc-link voltage, but it can be handled by the motor electronics. Figure 1(b) directly interfaces batteries with the motor drive dc-link. Ultracapacitors take over the transient power via a bi-directional dc/dc converter. This configuration is best suited for battery powered electric vehicles. In this paper, the configuration (a) is

modeled in detail. The use of two bi-directional dc/dc converters to control the power flow in/out of the battery and ultracapacitor is possible and is the most flexible, but it is the most costly with likely minimal gain in system performance.
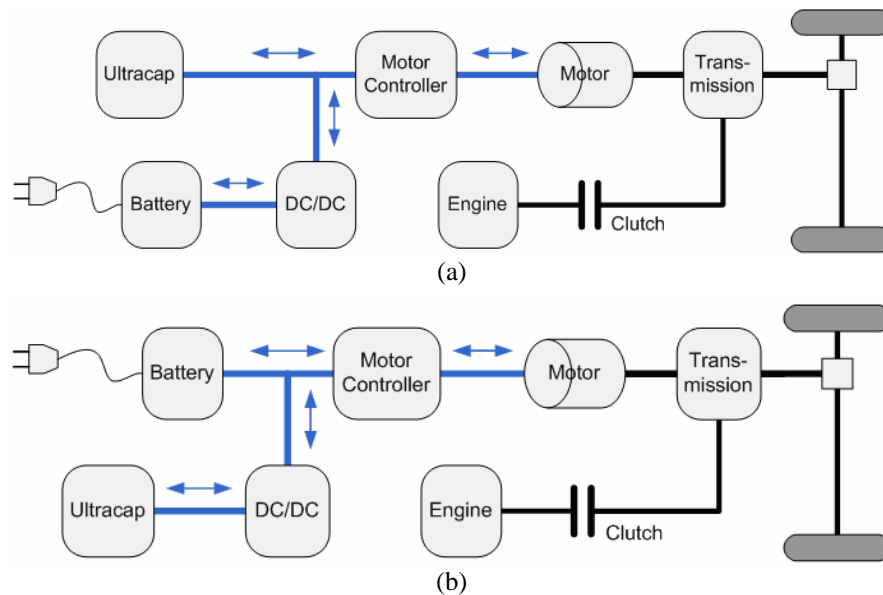

(a)

(b)

Figure 1: Driveline Configurations of PHEVs Combining Batteries and Ultracapacitors

In the PHEV model with two energy storage units, there are three basic driveline operating modes: (1) EV mode (electric drive only), (2) HEV mode with optimal engine operation, and (3) HEV mode with normal engine operation. These various modes are shown in Figure 2. In terms of the batteries, there are two modes: (1) a charge depleting mode in which the battery state-of-charge is decreasing to a specified minimum value, (2) a charge sustaining mode that maintains the minimum state-of-charge of the battery utilizing the engine and motor/generator as in the Toyota Prius and Honda hybrid Civic.
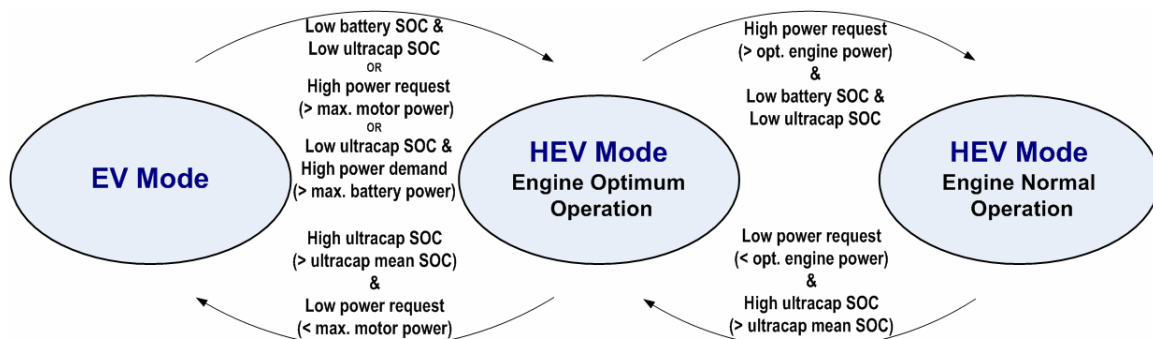

Figure 2: Modes of operation of the PHEV with two energy storages

In the EV mode, only the traction motor powers the vehicle. Batteries and/or ultracapacitors supply or absorb power up to the limits of the traction motor. Batteries provide the time-averaged power and the ultracapacitor provides the remainder of the power needed by the vehicle. This reduces stress on the battery and extends battery life. For a PHEV, most of this operation takes place in the battery charge depleting mode at vehicle ranges less than AER. The ultracapacitor is controlled to be within its appropriate voltage limits via charging from the battery when needed and it accepts all the regenerative braking energy.

In this mode, a 90sec moving average is used to smooth the battery power. The maximum power of the battery is limited to one third of the maximum power of the traction motor. To limit the voltage swing of

ultracapacitors (traction motor dc-link), the minimum voltage of the ultracapacitor is set to 50 percent of the maximum, rated voltage (The usable energy is 75 percent of the total energy stored in the capacitor), and the ultracapacitor *SOC* is controlled between 0.2 and 0.9.

In HEV mode with optimal engine operation, the engine runs near maximum efficiency at all engine speeds and provides the resultant optimum power regardless of the power demand of the vehicle. In order to balance the engine output power with that required by the vehicle, the difference via the motor/generator is either absorbed or provided by the ultracapacitor. This mode of operation occurs most frequently in the battery charge sustaining mode near minimum battery state-of-charge. In this mode, the intent is to provide all electrical power from the ultracapacitors and have them accept all the regenerative braking energy. The battery is not used unless the ultracapacitor would happen to be completely depleted.

In HEV mode with normal engine operation, the engine provides the required vehicle propulsion power as in a conventional vehicle and charges the ultracapacitor if needed.
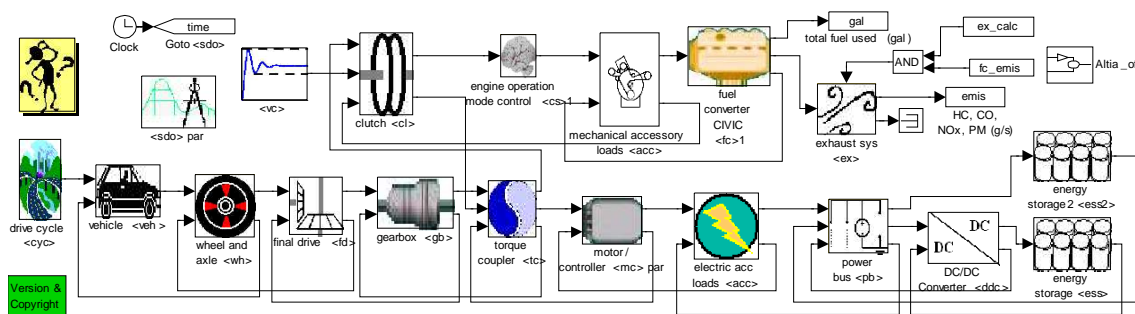

Figure 3: Advisor vehicle block diagram

The block diagram for the PHEV vehicle simulation in *Advisor* is shown in Figure 3. As indicated by the previous discussion of the various operating modes of the vehicle, the control of the PHEV is quite complex as it involves minimizing the stress on the battery and optimizing the efficiency of engine operation using the high power, high efficiency ultracapacitor as an electrical energy buffer and for recovery of energy from regenerative braking. In addition, the control strategy must be applicable to the various driving cycles (FUDS, Fed Highway, and US06) that vary significantly in their power demand characteristics. The simulation results of the next section will show large differences as to how the energy storage units respond to vehicle operation on the various driving cycles.

Simulation Results for PHEVs Using Batteries and Ultracapacitors

Vehicle design parameters and electric and engine characteristics

All the simulations were performed using the following vehicle inputs:
$C_D = .27$, $A_F = 2.2$ m^2, $f_r = .008$, test weight = 1650 kg (approx.)
Engine: Honda 1.3L, iVTEC engine map, scaled to 90 kW
Electric motor: Honda hybrid Civic AC PM 2006 efficiency map, scaled to 70 kW
DC/DC inverter: constant efficiency 0.96
Transmission: 5-speed manual (3.11, 2.11, 1.55, 1.0, .71, FD=3.95), automatically shifted in the model, but future models would incorporate the DCT (dual clutch transmission) as a convenient means to have smooth, fast shifting and to decouple the engine when it is not needed to provide power.

Batteries and ultracapacitors

Simulations were performed using batteries and ultracapacitors with the characteristics shown in Table 3. The weights of the energy storage units are given in terms of the weights of the cells in the various units.

The weights of the complete units would be higher due packaging and unit management considerations, but the performance of the unit is dependent on the cell weights. The energy storage unit cell weights used in the simulations are the following:

Lithium-ion batteries
EIG NiCoMnO$_2$	30 kg	20 Ah cells	60 in series	3.5 kWh useable
Composite MnO$_2$	32 kg	40 Ah cells	60 in series	4.6 kWh useable
Silicone composite	22 kg	30 Ah cells	60 in series	4.6 kWh useable

Zinc-air batteries
Zn-air	32 kg	60Ah cells	180 in series	9.5 kWh useable

Carbon/carbon ultracapacitors
Symmetric C/C	20 kg	1350F cells	110 in series	100 Wh useable

The nominal energy storage unit voltage was 240V (approx.) in all cases with the maximum currents limited to about 300A even in the cases of the batteries alone. In all cases, the batteries were depleted to 30% SOC from 100% SOC.

Simulation results and their interpretation

Computer runs were performed for PHEVs using the batteries shown above with and without the ultracapacitors. Simulations were made for the FUDS, Fed Highway, and US06 driving cycles. For each of the driving cycles, runs were made for selected numbers of cycles to represent driving in the charge depleting and charge sustaining modes of operation. The all-electric range (AER) and electric energy use (Wh/mi) were determined for the charge depleting mode and the fuel economy (mpg) was determined for all cases/modes in which the engine was operating. The simulation results are summarized in Tables 6 for the battery and ultracapacitor combinations and in Table 7 for the cases of batteries alone without ultracapacitors.

With the batteries in combination with the ultracapacitors, the PHEVs were able to operate in the all-electric mode until the battery SOC=30% on the FUDS and Fed Highway driving cycles. In all cases for the US06 driving cycle, the vehicle had blended operation (engine and electric drive both needed) in the charge depleting mode. The use of the ultracapacitors with the batteries permits all-electric operation of the vehicle have a wide range of driving conditions and higher Wh/mi for all the driving cycles. Hence in the charge depleting mode, the fuel economy (mpg) is higher by 50-100% using the ultracapacitors for all the batteries. The fuel economy in the charge sustaining mode is also higher for all the driving cycles using the ultracapacitors, but only by 15-40% in most cases. The acceleration times of the vehicle were lower using the ultracapacitors than for the batteries alone. With the ultracapacitors, the acceleration times were 2.7 sec for 0-30 mph and 6.9 sec for 0-60 mph. For the batteries alone, the acceleration times varied somewhat with the battery used ranging from 2.9-3.2 sec for 0-30 mph and 8.6-9.8 sec for 0-60 mph. Hence in all respects, vehicle performance was improved using the ultracapacitors for all the batteries studied.

The current and voltage responses of the batteries with and without the ultracapacitors are shown in Figures 4-7 for the silicone carbon lithium-ion and the Zinc-air batteries for the FUDS and US06 driving cycles. The effects of the load leveling of the power demand from the batteries using the ultracapacitors are clearly evident in the figures. Both the average currents and the peak currents from the batteries are lower by a factor of 2-3 using the ultracapacitors. The minimum voltages of the batteries are significantly higher using the capacitors and the voltage dynamics (fluctuations) are dramatically reduced. Hence the stress on the battery and resultant heating are much reduced. The simulation results in Figures 4-7 also show that the ultracapacitors are utilized over a wide voltage range indicating that a large fraction of their usable energy storage (100 Wh) is being used to load level the batteries. This is only possible using a DC/DC converter between the battery and the DC- bus.

The simulation results also indicate that using ultracapacitors, batteries with a wide range of power characteristics can be used in PHEVs and also EVs without sacrificing vehicle performance and subjecting the batteries to high stress and resultant shorter cycle life. This could be especially important in the future as high energy density batteries such as Zinc-air and possibly lithium-air are developed. It is likely that

those battery types will not have commensurate increases in useable power density and without ultracapacitors, the battery unit in PHEVs and EVs would be sized by the maximum power requirement (kW) rather than the range (mi)/energy requirement (kWh). This would significantly increase weight, volume, and the cost of the battery unit. It is also unlikely that the air electrode will have charge acceptance capability and thus regenerative braking performance approaching that of ultracapacitors or even lithium-ion batteries. This is another advantage of the use of ultracapacitors with the air-electrode batteries.

Table 6: Simulation results for the advanced batteries with ultracapacitors

Battery Type (1)	cycle	Range mi.	kW max. control	kW max bat.	Eff. Bat.	kW max. Cap.	Eff. Cap.	Wh/mi Bat.	Operat. mode	mpg 20mi	mpg 40mi	Ch. Sus. HEV mpg
Compos. MnO2	FUD	22	40	18	.94	40	.97	215	AE	none	97	52.8
32kgbat	HW	20	45	18	.91	45	.96	227	AE	none	109	56.3
20kgcap	US06	30	68	21	.91	68	.94	180	blended	71.9	56	38.3
Si Carb/ Compos. MnO2	FUD	20	40	18	.94	40	.97	220	AE	none	99	52.8
22kgbat	HW	20	45	19	.91	45	.97	225	AE	none	110	56.8
20kgcap	US06	30	68	21	.91	68	.94	190	blended	71.1	52	38.4
Rech. Zn-air	FUD	40	45	19	.87	45	.97	228	AE	none	none	54.5
32kgbat	HW	38	45	19	.81	45	.97	242	AE	none	none	57.7
20kgcap	US06	66	68	21	.82	68	94	149	blended	62.4	60	38.8

(1) weight of cells only

Table 7: Simulation results for the batteries alone

Battery Type (1)	cycle	Range mi.	kW max. control.	kW max. bat.	Eff. Bat.	Wh/mi Bat.	Operat. mode	mpg 20mi .	mpg 40mi	Mpg Ch. sus. HEV
EIG NiCoMn	FUD	27	30	30	.94	125	blended	134	85	47
30 kg	HW	24	20	20	.93	137	blended	110	87	47
	US06	57	58	58	.88		blended	48	45	37
Compos. MnO2	FUD	36	30	30	.92	135	blended	134	104	46.9
32kgbat	HW	31	20	20	.91	147	blended	167	113	46.6
	US06	64	58	58	.87	92	blended	48	48	34.1
Si Carb/ Compos. MnO2	FUD	35	30	30	.93	138	blended	138	106	46.9
22kgbat	HW	32	20	20	.92	148	blended	169	114	46.9
	US06	64	58	58	.88	87	blended	48	48	35.7
Rech. Zn-air	FUD	66	30	30	.84	139	blended	139	137	39.4
32kgbat	HW	63	20	20	.83	156	blended	169	169	41.1
	US06	93	36	36	.72	101	blended	48.5	48.5	30.1

(1) weight of cells only

FUDS without ultracapacitors   FUDS with ultracapacitors
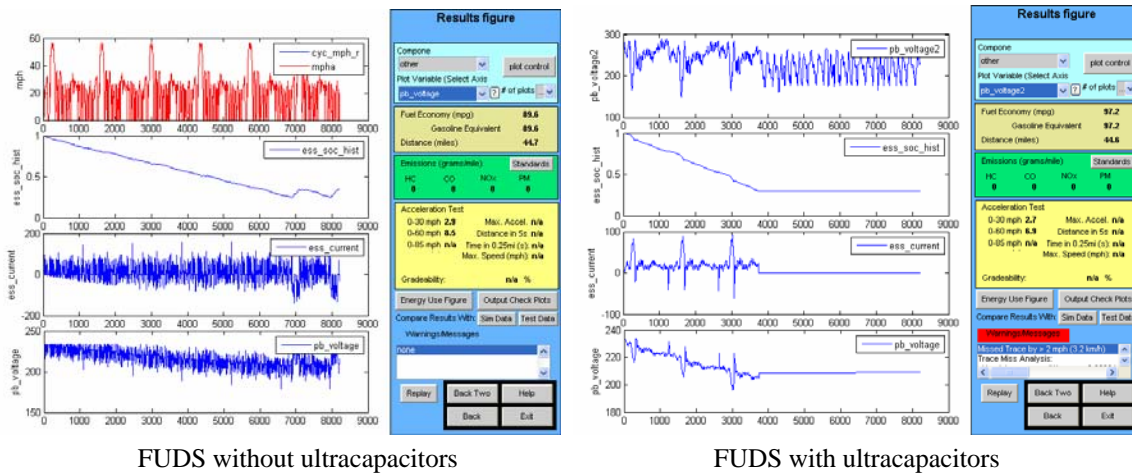
Figure 4: The Si Carbon lithium battery on the FUDS with and without ultracapacitors

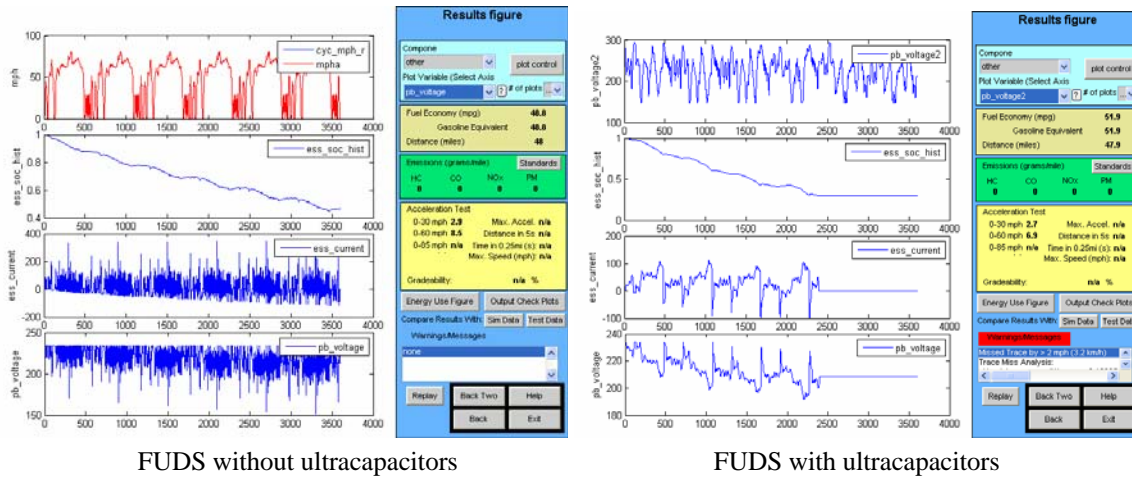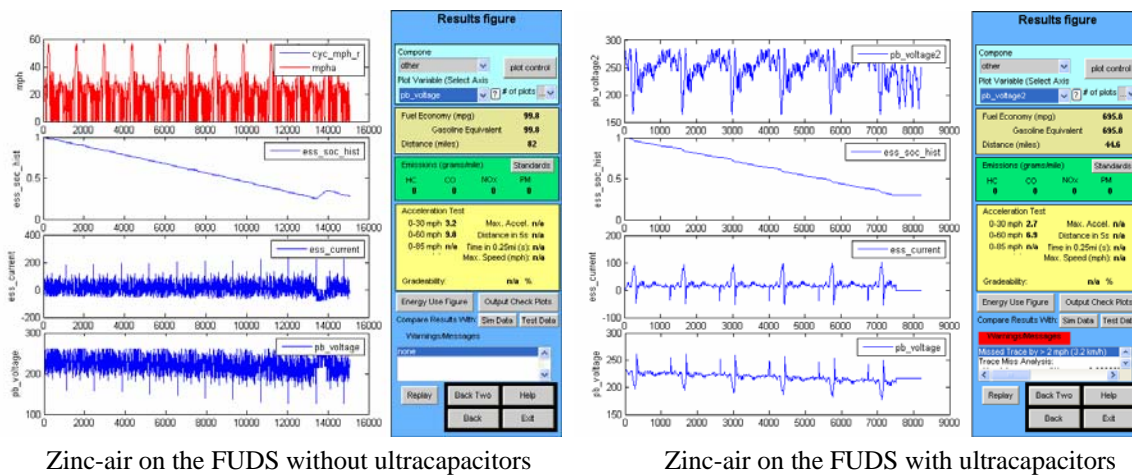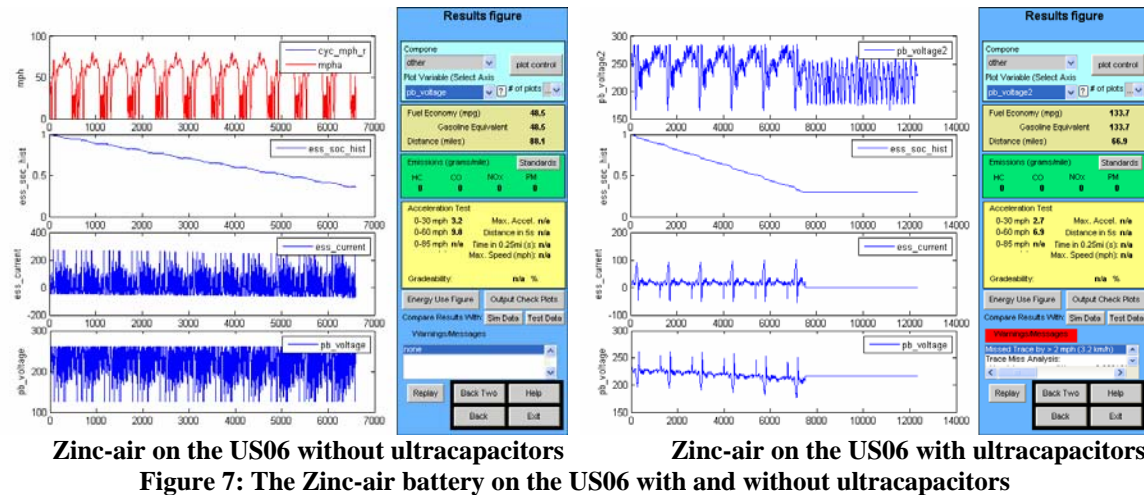FUDS without ultracapacitors   FUDS with ultracapacitors

Figure 5: The Si Carbon lithium battery on the US06 with and without ultracapacitors

Zinc-air on the FUDS without ultracapacitors   Zinc-air on the FUDS with ultracapacitors

Figure 6: The Zinc-air battery on the FUDS with and without ultracapacitors

Zinc-air on the US06 without ultracapacitors **Zinc-air on the US06 with ultracapacitors**
Figure 7: The Zinc-air battery on the US06 with and without ultracapacitors

Summary and Conclusion

This paper is concerned with the use of ultracapacitors in plug-in hybrid vehicles (PHEVs) in combination with high energy density lithium-ion (200-300 Wh/kg) and zinc-air batteries (400 Wh/kg). Battery energy density and power capability characteristics are assumed for use in new vehicle simulation models that include battery/ultracapacitor combinations for energy storage (2-energy storage systems and associated control strategies). These new models include a DC/DC inverter to control the energy flow from the battery and/or the ultracapacitors. The control strategies result in load leveling the batteries and having the ultracapacitors accept all the regenerative braking energy. The ultracapacitor characteristics used in the simulations are those of a symmetric, activated carbon device using acetonitrile as the electrolyte. The total weights of the cells in the lithium-ion batteries were 20-22 kg and in the zinc-air battery, 32 kg. The cell weight of the ultracapacitors was 20 kg. The all-electric range using the lithium batteries was 20 miles and 40 miles using the zinc-air battery.

Simulations were performed for the FUDS, Fed Highway, and US06 driving cycles with the PHEVs operating in both the charge depleting and charge sustaining modes. With the batteries in combination with the ultracapacitors, the PHEVs were able to operate in the all-electric mode until the battery SOC=30% on the FUDS and Fed Highway driving cycles. In all cases for the US06 driving cycle, the vehicle had blended operation in the charge depleting mode. In the charge depleting mode, the fuel economy (mpg) is higher by 50-100% using the ultracapacitors for all the batteries. The fuel economy in the charge sustaining mode is also higher for all the driving cycles using the ultracapacitors, but only by 15-40% in most cases. The acceleration times of the vehicle were lower using the ultracapacitors than for the batteries alone. With the ultracapacitors, the acceleration times were 2.7 sec for 0-30 mph and 6.9 sec for 0-60 mph. For the batteries alone, the acceleration times varied somewhat with the battery used ranging from 2.9-3.2 sec for 0-30 mph and 8.6-9.8 sec for 0-60 mph.

The effects of the load leveling of the power demand from the batteries using the ultracapacitors are clearly evident in the simulation results. Both the average currents and the peak currents from the batteries are lower by a factor of 2-3 using the ultracapacitors. The minimum voltages of the batteries are significantly higher using the capacitors and the voltage dynamics (fluctuations) are dramatically reduced. Hence the stress on the battery and resultant heating are much reduced. The simulation results also show that the ultracapacitors are utilized over a wide voltage range indicating that a large fraction of their usable energy storage (100 Wh) is being used to load level the batteries. This is only possible using a DC/DC converter between the battery and the DC- bus.

The simulation results also indicate that using ultracapacitors, batteries with a wide range of power characteristics can be used in PHEVs and also EVs without sacrificing vehicle performance and subjecting the batteries to high stress and resultant shorter cycle life. This could be especially important in the future as high energy density batteries such as Zinc-air and possibly lithium-air are developed. It is likely that those battery types will not have commensurate increases in useable power density and without ultracapacitors, the battery unit in PHEVs and EVs would be sized by the maximum power requirement (kW) rather than the range (mi)/energy requirement (kWh). This would significantly increase weight, volume, and the cost of the battery unit.   It is also unlikely that the air electrode will have charge acceptance capability and thus regenerative braking performance approaching that of ultracapacitors or even lithium-ion batteries. This is another advantage of the use of ultracapacitors with the air-electrode batteries.

References

1. Burke AF, Van Gelder E. Plug-in Hybrid-Electric Vehicle Powertrain Design and Control Strategy Options and Simulation Results with Lithium-ion Batteries. EET-2008 European Ele-Drive Conference, Geneva, Switzerland, March 12, 2008.

2. Burke AF, Zhao H, Van Gelder E. Simulated Performance of Alternative Hybrid-Electric Powertrains in Vehicles on Various Driving Cycles. EVS-24, Stavanger, Norway, May 2009.

3. Zhao, H. and Burke, A.F., Optimization of fuel Cell System Operating Conditions for Fuel cell Vehicles, Journal of Power Sources, Vol.186, Issue 2 (2009),408-416

4. Burke, A.F. and Miller, M., The UC Davis Emerging Lithium Battery Test Project, Report UCD-ITS-RR-09-18, July 2009

5. Burke, A.F. and Miller, M., Performance Characteristics of Lithium-ion Batteries of Various Chemistries for Plug-in Hybrid Vehicles, EVS-24, Stavanger, Norway, May 2009 (paper on the CD of the meeting)

6. Burke, A.F. and Miller, M., Electrochemical Capacitors as Energy Storage in Hybrid-Electric Vehicles: Present Status and Future Prospects, EVS-24, Stavanger, Norway, May 2009 (paper on the CD of the meeting)

7. Burke, A. and Miller, M., Supercapacitors for Hybrid-electric Vehicles: Recent Test Data and Future Projections, Advanced Capacitor World Summit 2008, San Diego, California, July 14-16, 2008

8. Thackeray, M.M., etals, Li_2MnO_3-stablized $LiMnO_2$ (M=Mn, Ni, Co) electrodes for lithium-ion batteries, Journal of Materials Chemistry, 2007, 17, 3112-3125

9. DOE Annual Merit Review and Pier Evaluation Meeting, Hydrogen Program and Vehicle Technology Program, May 18-22, 2009, Washington, D.C., papers on the CD for the meeting under electrochemistry programs

10. Yang, X., etals, Synthesis and electrochemical properties of novel silicon-based composite anode for lithium-ion batteries, Journal of Alloys and Compounds, Volume 464, September 2008, pages 265-269

11. Holzapfel, M., etals, Nano silicon for lithium-ion batteries, Electrochimica Acta, Vol 52, November 2006, pages 973-978

12. Revolt Portable Battery – Technology Brief, white paper taken from the Revolt Techology website, www. Revolttechnology.com

13. S. Pay, and Y. Baghzouz, Effectiveness of Battery-Supercapacitor Combination in Electric Vehicles, 2003 IEEE Bologna Power Tech Conference, June 23th-26th, Bologna, Italy

14. Jonathan J. Awerbuch and Charles R. Sullivan, Control of Ultracapacitor-Battery Hybrid Power Source for Vehicular Applications, IEEE Conference on Global Sustainable Energy Infrastructure: Energy2030, Nov. 17-18, 2008

15. Shuai Lu, Keith A. Corzine, and Mehdi Ferdowsi, A New Battery/Ultracapacitor Energy Storage System Design and Its Motor Drive Integration for Hybrid Electric Vehicles, IEEE Transactions on Vehicular Technology, Vol. 56, No. 4, July 2007, 1516-1523

16. Burke, A.F., Miller, M., and Van Gelder, E., Ultracapacitors and Batteries for Hybrid Vehicle Applications, 23rd Electric Vehicle Symposium, Anaheim, California, December 2007 (paper on CD of proceedings)

17. Burke, A.F., Cost-Effective Combinations of Ultracapacitors and Batteries for Vehicle Applications, Proceedings of the Second International Advanced Battery Conference, Las Vegas, Nevada, February 4-7, 2002

18. Miller, J.M., Active Combinations of Ultracapacitor-Battery Energy Storage Systems Gaining Traction, Proceedings of the 19th International Seminar on Double-layer Capacitors and Hybrid Energy storage Devices, Deerfield Beach, Florida, December 2009

19. Miller, J.M., Energy Storage System Technology Facing Strong Hybrids, Plug-in and Batttery Electric Vehicles, The 5th IEEE Vehicle Power and Propulsion Conference, VPPC2009, Dearborn, Michigan, Sept 7-10, 2009

20. Miller, J.M., Bohn, T., Dougherty, T., and Deshpande, U., Why Hybridization of Energy Storage is Essential for Future Hybrid Plug-in and Battery Electric Vehicles, The 1st IEEE Energy conversion Congress and exposition, ECCE2009, San Jose, California, Sept 21-24, 2009